Chemical Engineering Journal 382 (2020) 123040

Contents lists available at ScienceDirect

Chemical Engineering Journal

journal homepage: www.elsevier.com/locate/cej

Arsenite simultaneous sorption and oxidation by natural ferruginous manganese ores with various ratios of Mn/Fe

Lin Ma[a,b,1], Dongmei Cai[c,1], Shuxin Tu[c,*]

[a] Key Laboratory of Aquatic Botany and Watershed Ecology, Wuhan Botanical Garden, Chinese Academy of Sciences, Wuhan 430074, PR China
[b] Center of Plant Ecology, Core Botanical Gardens, Chinese Academy of Sciences, Wuhan 430074, PR China
[c] College of Resources and Environment, Huazhong Agricultural University, 430070 Wuhan, PR China

HIGHLIGHTS

- As(III) sorption and oxidation by natural ferruginous manganese ores are studied.
- The NFMO with high Mn: Fe ratio had stronger oxidation capacity for As(III).
- The As(III) adsorption efficiency of NFMOs increased with Fe content increasing.
- Pyrophosphate formed the complexes with Mn(III) was favor for As(III) oxidation.
- Mn/Fe oxides are responsible for the As(III) oxidation and sorption, respectively.

GRAPHICAL ABSTRACT

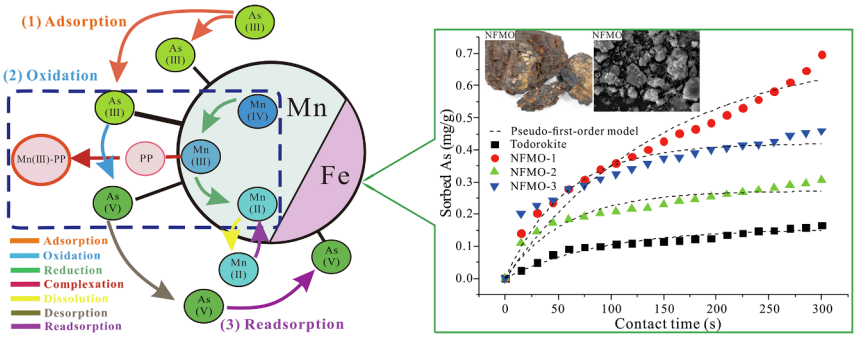

ARTICLE INFO

Keywords:
Natural ferruginous manganese ore
Arsenite
Adsorption
Oxidation
Pyrophosphate

ABSTRACT

Arsenite [As(III)], is more toxic and difficult to remove from aqueous systems compared to arsenate [As(V)], and as such poses a significant health risk to humans and the environment. In order to make it more amenable to efficient removal, an oxidation pre-treatment of As(III) is particularly important. Compared to synthetic adsorbents, the low cost and abundance of natural ferruginous manganese ore (NFMO), make it a potentially attractive adsorbent for application in large-scale treatments. Here, we investigated the simultaneous oxidation and adsorption behaviour of As(III) with three NFMOs, each consisting of different Mn/Fe molar ratios. Results demonstrated that the NFMO with a high Mn:Fe ratio had a stronger oxidation capacity for As(III), while As(III) adsorption efficiency of NFMOs increased with increasing Fe content. The sorbent dosage was an important factor for As(III) oxidation with NFMOs having higher Mn contents, but not for ores with low contents. An pH increasing from 6 to 7.9 enhanced the As(III) oxidation by NFMOs. Furthermore, the As(III) oxidation rate of NFMO increased by 68% with the addition of pyrophosphate (PP), and increasing PP concentrations led to higher oxidation rates. During the process, PP formed complexes with Mn(III), thus accelerating the conversion of Mn(IV) to Mn(III). Later, the dissolution of these complexes led to a generation of additional oxidation adsorption sites, favouring As(III) oxidation. FTIR and XPS analyses further confirmed that reduction of Mn(IV) and Mn(III) species played a vital role in the oxidation of As(III) to As(V). As(III) removal by NFMO was attributed to the joint effect of sorption and oxidation processes, where Manganese oxide was responsible for As(III) oxidation, while Fe oxide played a primary role in the arsenic sorption.

* Corresponding author at: College of Resources and Environment, Huazhong Agricultural University, 430070 Wuhan, PR China.
E-mail address: stu@mail.hzau.edu.cn (S. Tu).
[1] The first two authors contributed equally to this work.

https://doi.org/10.1016/j.cej.2019.123040
Received 6 August 2019; Received in revised form 30 September 2019; Accepted 1 October 2019
Available online 10 October 2019
1385-8947/

1. Introduction

Arsenic (As) is considered a highly toxic and carcinogenic element, whose contamination in aqueous systems has attracted extensive attention, globally [1,2]. Elevated concentrations of As in aquatic environments are attributed to both natural processes and anthropogenic activities [3,4]. Long-term uptake of water contaminated with arsenic can result in the development of cancer and other severe health problems in humans. [5,6]. To minimise public health risks, many countries have adopted a stringent As limit of 10 μgL^{-1} in drinking water provided by the World Health Organization (WHO).

In natural waters, soluble As occurs predominantly in two species, arsenate [As(V)] and arsenite [As(III)]. As(III) is considered to be more toxic, soluble, mobile, and difficult to remove than As(V) [1,7]. Numerous methods have been developed to remove As from water [8,9], of which adsorption is widely regarded as the most promising approach, owing to its high efficiency and cost-effectiveness [10,11]. A series of studies has been conducted on As extraction from water using various metal oxide sorbents [12,13]. However, most sorbents are effective for As(V) removal, but fail in the case of As(III). This is mainly due to the low affinity of arsenous acid (H_3AsO_3) for the sorbent surface at low concentrations [14]. Hence, preceding sorption, an oxidation pretreatment is usually employed for the conversion of As(III) to As(V) [15].

Manganese oxides have been extensively used as oxidising agents for specific oxidation of As(III) [16,17]. However, the adsorption capacity of pure manganese oxide (MnO_2) for As is relatively low, limiting its application [18]. Recently, an Fe–Mn binary oxide adsorbent has been shown as highly effective for both As(V) and As(III) removal, especially for the latter [7,19–22]. This material combines oxidation properties of MnO_2 with the high adsorption capability of iron oxides, consequently being highly effective in simultaneously removing As(V) and As(III). Previous studies on As sorption onto nature ferruginous manganese ore (NFMO) are relatively few [23,24]. Most investigations have focused on synthetic Fe–Mn binary oxides [25,26], even though compared to these synthetic adsorbents, low-cost NFMOs are more suitable for large-scale applications. It is well-known that Mn/Fe ratios vary greatly in NFMOs [27], which in turn influence As uptake considerably. Therefore, unveiling NFMO oxidation and adsorption of As (III), its behaviour and inherent mechanism can contribute to a comprehensive understanding of the fate and transport of As in natural environments.

Pyrophosphate (PP), a particularly effective chelating agent, is shown to form strong complexes with Mn(III) at neutral pH [28]. In recent years, a lot of attention has been devoted to Mn(III)-PP complexes, as they are an important aspect of manganese cycles in natural water [29–31]. However, little consideration has been given to the possible effects of Mn(III) complexes on NFMO arsenite oxidation in natural waters. Interactions between Mn(III) and PP may reduce the formation of Mn (II), consequently increasing the number of available oxidation-adsorption sites on mineral surfaces for H_3AsO_3, and promoting As(III) oxidation by Fe–Mn binary oxides [32,33].

In this study, we investigated As(III) oxidation and adsorption by three NFMOs with different Mn/Fe ratios. We hypothesised that ratios of manganese oxides and iron oxides would influence the efficiency of As removal from water. As such, our study had several purposes, namely: (1) comparing the three NFMO adsorption performances and oxidation kinetics of As(III) with various Mn/Fe ratios; (2) investigating As(III) oxidation behaviours as affected by sorbent dosage, solution pH and PP addition; (3) revealing the mechanisms of simultaneous As oxidation and adsorption by NFMOs through XRD and XPS characterisation.

2. Materials and methods

2.1. Chemicals

All chemicals were of analytical grade and used without further purification. As(III) and As(V) stock solutions were prepared by dissolving $NaAsO_2$ (Xiya Chemical industry, Co. Ltd, Shandong, China) and $Na_3AsO_4{\cdot}12H_2O$ (Sinopharm Chemical Reagent Co. Ltd, Shanghai, China) respectively, in ultrapure water. Arsenic working solutions were freshly prepared by diluting appropriate amounts of As stock solution with deionised water. Pyrophosphate ($Na_4P_2O_7{\cdot}10H_2O$) and antimony potassium tartrate ($KSbC_4H_4O_7{\cdot}1/2H_2O$) were obtained from Hushi Chemical industry, Co. Ltd, (Shanghai, China) and Kaitong chemical reagent Co. Ltd (Tianjin, China), respectively. Background electrolyte solution contained 10 mmol/L of NaCl and 5 mmol/L of MOPS. All additional chemicals were purchased from Sinopharm Chemical Reagent Co., Ltd. (Shanghai, China).

2.2. Adsorbent preparation and characterisation

The NFMO Mn/Fe molar ratios were 31.94:1 (38.33% Mn and 1.20% Fe), 4.88:1 (33.49% Mn and 6.86% Fe), and 2.20:1 (20.93% Mn and 9.51% Fe), termed as NFMO-1, NFMO-2, and NFMO-3, respectively. For the control, we synthesised a todorokite (52.89% Mn and 0% Fe), by a reflux method, according to a literature procedure [34].

Mn average oxidation states (AOS) of NFMO were analysed using a sodium oxalate-potassium permanganate back titration method [35]. The point of zero charge (PZC) was measured by a modified salt titration method [36]. NFMO pH and moisture content were determined as previously described [7,21]. Adsorbent constituents were estimated with an X-ray fluorescence spectrometer (XRF Axios advanced, PANalytical B.V.) and particle images were observed on a scanning electron microscope (SEM VEGA 3 XMU, Tescan). X-ray diffraction (XRD) patterns of powder samples from NFMOs were carried out on a Bruker D8 Advance (Germany) with CuK radiation. Fourier transform infrared (FTIR) spectra were collected on a BrukerEqulnox55 FTIR spectrophotometer (Bruker Co., Germany) using a transmission model. Samples for FTIR determination were ground with spectral grade KBr in an agate mortar. X-ray photoelectron spectra (XPS) were analysed by an ESCALab-220i-XL spectrometer with a monochromatic Al Kα X-ray source (1486.6 eV). C1s peaks were used as an inner standard calibration peak at 284.7 eV. Specific Surface Area (SSA), pore volume, and average pore size were determined via nitrogen adsorption using the BET method with a Micromeritics ASAP 2000 surface area analyser (Micromeritics Co., USA).

2.3. Batch adsorption tests

2.3.1. Adsorption performance

In order to compare adsorption capacities of NFMOs with different Mn:Fe molar ratios, we performed batch experiments for As(III) or As (V) (30 mL, 500 μmol/L) under a fixed NFMO-1, −2 or −3 dose of 0.20 g. Mixtures were loaded into 100-ml centrifuge tubes, followed by addition 30 mL of background electrolyte solution. Samples were then stirred on a shaker at 250 rpm and 25 °C for 24 h. During the shaking process, pH was maintained at 7 ± 0.05 by addition 0.1 M HCl or NaOH. After 24 h, all samples were centrifuged at 8000 rpm and 25 °C for 10 min, and the supernatants were collected for As analysis. Concentrations of total As and As(III) species were determined by atomic fluorescence spectrometry (AFS-9700), as previously described [37]. The As(V) concentration was obtained by subtracting the As(III) concentration from the total As concentration.

2.3.2. Reaction kinetics

Kinetics experiments were conducted in batches in order to determine the oxidation rate of As(III). NFMO-1, −2 or −3 (1.00 g) was added to a 500 mL glass vessel containing As(III) (150 mL, 500 μmol/L), and 150 mL of background electrolyte solution. This mixture was stirred on a shaker at 250 rpm and 25 °C for 24 h. Throughout the experiment, pH was maintained at 7 ± 0.05 by addition of 0.1 M HCl or NaOH. Aliquots of ca. 4 mL were taken from the suspensions at the following intervals: every 15 s for the first 5 min, then at 7, 10, 15, 20, 24, 29, 35, 42, 50, 59 and 69 min. Samples were immediately centrifuged and analysed.

2.3.3. Effect of sorbent dosage and pH on As(III) oxidation

To investigate the effect of sorbent dosage and pH on As(III) oxidation, all batch tests were carried out in 500 mL glass vessels, containing As(III) (150 mL, 500 μmol/L) and 150 mL of electrolyte solution. Addition of 0.15, 0.50, or 1.00 g of NFMO-1, −2 or −3 to was then executed and pH was adjusted to 6, 7, or 7.9 with dilute HNO_3 and/or NaOH solution. Reactions were stirred on a shaker at 250 rpm and 25 °C. Aliquots of ca. 4 mL were collected from the suspension at 0, 1, 2, 3, 5, 7, 10, 15, 20, 24, 29, 35, 42, 50, 59, and 69 min. After 24 h, samples were analysed as described in Section 2.3.1.

2.3.4. Influence of pyrophosphate on As(III) oxidation

Effects of two different PP addition protocols as well PP concentration on As (III) oxidation efficiency were studied. In the first protocol, NFMO-2 (1.00 g) was suspended in $Na_4P_2O_7$ solution (150 mL, 5 mmol/L, pH = 7) at 25 °C for 12 h; then As (III) solution (150 mL, 500 μmol/L) was added into the mixture. In the second, NFMO-2 (1.00 g) was suspended in 150 mL of electrolyte solution at 25 °C for 12 h; to this mixture was added As(III) solution (150 mL, 500 μmol/L), containing $Na_4P_2O_7$ (150 mL, 5 mmol/L, pH = 7).

To determine the influence of PP concentration on As(III) oxidation, batch tests were performed. First, NFMO-2 (1.00 g) was dispersed in 150 mL of electrolyte solution at 25 °C for 12 h. Then, As(III) (150 mL, 500 μmol/L) solutions each containing $Na_4P_2O_7$ (1, 2.5 or 5 mmol/L), were added to the suspensions.

All batch solutions contained background electrolyte solution to maintain a relatively constant ionic strength. Suspensions were shaken on an orbit shaker at 250 rpm at 25 °C and pH was adjusted with NaOH and/or HNO_3 solutions during the experiment. Aliquots of ca. 4 mL were taken from the mixtures at 0, 1, 2, 3, 5, 7, 10, 15, 20, 24, 29, 35, 42, 50, 59, and 69 min. In addition, we studied the effects of PP on As (III) oxidation within 5 h to investigate the continuous influence of pyrophosphate on the As(III) oxidation. Samples were immediately centrifuged and analysed for As, total Mn, and total Fe.

2.3.5. Analytical methods

All batch adsorption experiments were performed in triplicate and experimental blanks were run in parallel. Samples were analysed within 24 h of collection. Aqueous samples were acidified with concentrated HNO_3 in an amount of 1%, and stored in acid-washed glass vessels prior to analysis.

3. Results and discussion

3.1. NFMO characterisation

XRD patterns (Fig. S1) of the three NFMOs showed poorly ordered 2-line magnetite Fe_3O_4 and lepidocrocite γ-FeOOH patterns, with peaks at approximately 9° and 21°, respectively (PDF No. 01-079-0416, 00-052-1449). Meanwhile, three broad peaks at 19°, 28° and 37° were typical of pyrolusite phase β-MnO_2, and Mn_5O_8 (PDF No. 01-072-1982, 00-039-1218). Low-intensity peaks at approximately 33° and 42° were most likely those of Fe-Mn binary oxides (PDF No. 01-089-7073). The mineral phase presented in todorokite is pyrolusite [38].

Table 1
The chemical and physical properties of synthetical todorokite and NFMOs.

	Todorokite	NFMO-1	NFMO-2	NFMO-3
Mn content (%)	52.89	38.33	33.49	20.93
MnO_2 (%)	12.01	11.21	10.68	6.03
Fe content (%)	–	1.20	6.86	9.51
Mn: Fe molar ratio	–	31.94	4.88	2.20
AOS	3.65	3.77	3.43	3.51
Moisture content (%)	4.68	4.21	2.12	3.06
PZC	3.56	3.53	6.35	4.27
pH	6.95	6.89	7.04	6.80
SSA (m^2/g)	99.91	14.39	24.41	45.86
Pore volume (cm^3/g)	0.42	0.04	0.06	0.08
Average pore size (nm^2)	16.78	11.97	9.27	6.82

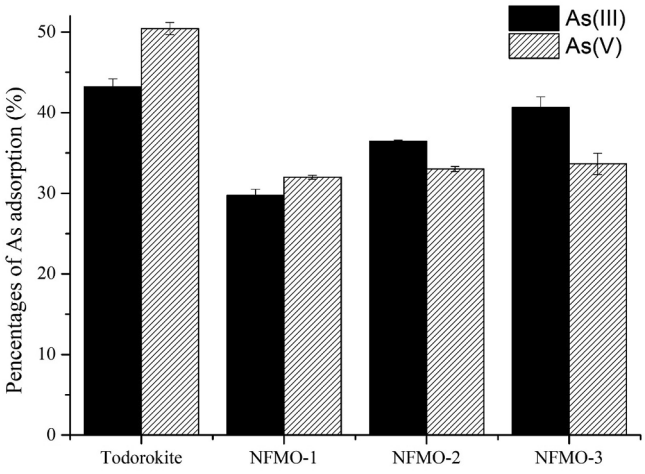

Fig. 1. Comparison of arsenic sorption by synthetical todorokite and NFMOs. Initial As(III)/As (V) concentration = 500 μmol/L, sorbent dosage = 0.20 g, pH = 7.0 ± 0.05, and T = 25 °C.

SEM images (Fig. S2) revealed that todorokite and NFMOs existed mainly in amorphous form, and were highly aggregated. XRF analysis illustrated that Fe and Mn were the most abundant elements present in all three NFMOs tested (Table 1). While only Mn was detectable in todorokite, with 12.01% MnO_2 content. AOS and pH of todorokite and NFMOs did not differ significantly, with a range of 3.4–3.8 and 6.8–7.0, respectively. The PZC values of todorokite, NFMO-1, NFMO-2, and NFMO-3 were 3.56, 3.53, 6.35, and 4.27, respectively (Table 1). A literature-reported pH_{PZC} value of 5.90 for Fe-Mn binary oxide with a 3:1 Mn/Fe ratio, falls between NFMO-3 and NFMO-2 Mn/Fe ratios (2.20:1 and 4.88:1, respectively) recorded in our study [7]. Moreover, todorokite and the NFMOs had specific surface areas of 14.39–99.91 m^2/g, lower than that of Fe-Mn binary oxides (265 m^2/g) [25]. Additionally, pore volumes of the four tested adsorbents were in a range of 0.0400–0.4188 cm^3/g, similar to that of Fe–Mn binary oxide incorporated into diatomite (0.025 cm^3/g) [39].

3.2. Adsorption performance

Arsenic adsorption efficiencies of three tested NFMOs were evaluated (Fig. 1). It was found that the percentage of As(III) adsorption increased with an increase in iron oxide content, being highest for NFMO-3 at 40.62%. While no significant differences were detected in the As(V) adsorption efficiencies for the three NFMOs, with an average value of 32.88%. The presence of Mn oxide would enhance As(III) uptake, and as an increase oxidation of As(III) compensated for the loss in As(III) sorption [21]. A previous study found that Fe-Mn binary oxide had a higher adsorption capacity toward As(V) than that of pure MnO_2 [40,41]. Hence, increasing iron oxide content enhances As(III) sorption,

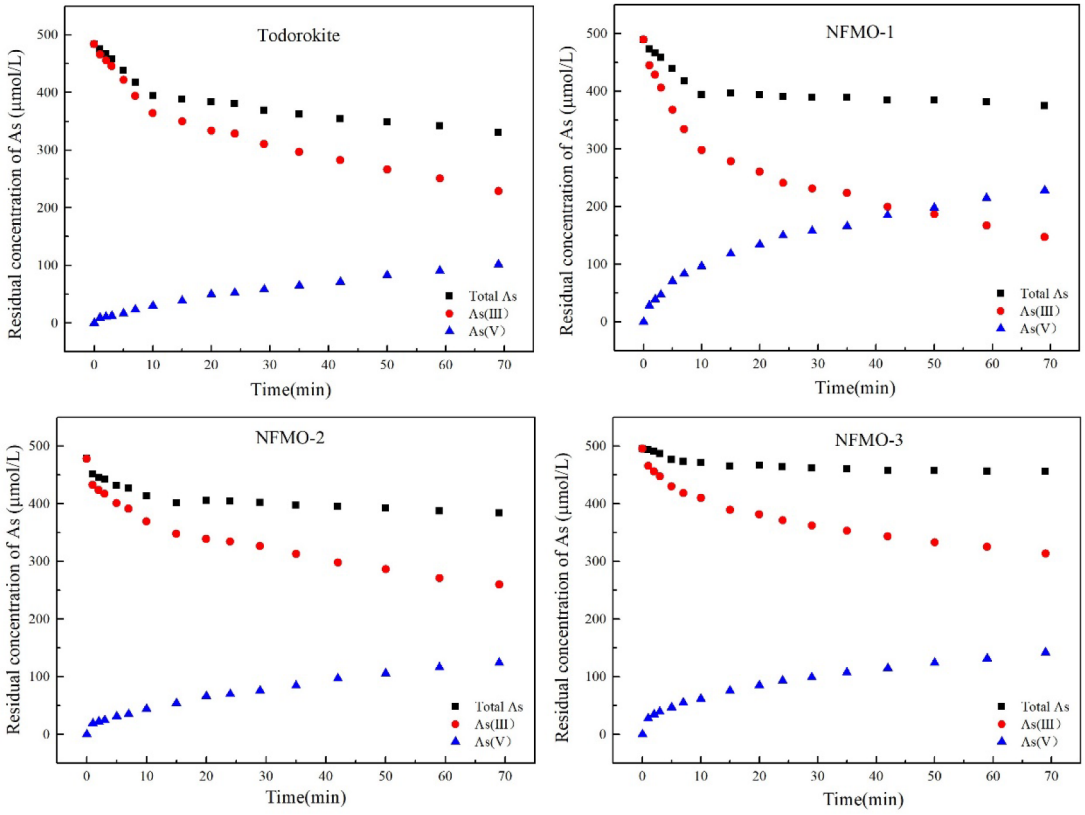

Fig. 2. The evolution of the aqueous concentration of arsenic species with reaction time at pH 7.0. Initial As(III) concentration = 500 μmol/L, sorbent dosage = 1.00 g, and T = 25 °C.

Table 2
Kinetic parameters for As(III) sorption on synthetical todorokite and NFMOs.

C_o = 500 μmol/L As(III)	External diffusion model					
	0–300 s			0–69 min		
	Kobs (min^{-1})	*K*($min^{-1}m^{-2}$)	R^2	*Kobs* (min^{-1})	*K*($min^{-1}m^{-2}$)	R^2
Todorokite	0.0242	0.0002	0.994	0.0103	0.0001	0.940
NFMO-1	0.0523	0.0036	0.994	0.0160	0.0011	0.921
NFMO-2	0.0185	0.0008	0.998	0.0078	0.0003	0.924
NFMO-3	0.0188	0.0004	0.987	0.0060	0.0001	0.903

especially when oxidizing As(III) to As(V). In addition, todorokite had a higher As(III) adsorption capacity due to its larger specific surface area compared to those of the NFMOs.

3.3. Reaction kinetics

Kinetic experiments were conducted to investigate NFMOs oxidation rate of As(III) from water. In a majority of previous kinetic studies of Fe-Mn binary oxide adsorbents, As(III) concentration reduces rapidly during the first hour, reaching an As(III) depletion of nearly 80% [6,25]. Meanwhile, according to previous reports, MnO_2 oxidation of As (III) proceeds rapidly in the first hour, especially within the initial 5 min. Therefore, in order to fully examine the kinetics, we focused on the oxidation dynamic within 5 min as well as at 70 min (Figs. 2 and S3). Oxidation rates of As(III) by NFMO-1, NFMO-2, NFMO-3, and todorokite were 49.2%, 26.8%, 32.8%, and 24.1% at 69 min, respectively, revealing that NFMO-1 had the highest oxidation capacity for As(III). This can be explained by higher AOS and Mn contents of NFMO-1 relative to that of the other absorbents tested.

As(III) was neutral at pH = 7, which was favourable for its diffusion from bulk solution into the solid phase. Since this bulk diffusion usually proceeded faster, analysis of the rate-determining step is generally estimated with an external diffusion model (EDM) [42]. As the focus was on the initial stages of As(III) oxidation kinetics, EDM was modified and expressed as: $\ln (C_t/C_0) = -K_{obs}\, t$, where C_0 and C_t (μmol/L) are As(III) concentrations at initial time, and any time t (min), respectively; K_{obs} and K are the apparent rate constant and apparent rate constant for per unit specific surface area, respectively. Reaction kinetics were accurately described by the EDM, evident from the proximity in values of determination coefficients (Fig. S4 and Table 2). Ginder-Vogel found that the EDM was suitable for fitting the oxidation process of As(III) by manganese oxide at initial 135–300 s, which is in agreement with our results [43]. Additionally, the higher K_{obs} value for NFMO-1 suggested that its As(III) oxidation rate is faster than that of the other absorbents, within a 70 min timeframe. K_{obs} values for all NFMOs were significantly higher in the initial five min compared to those within 69 min, confirming that As(III) underwent rapid oxidation within five min, followed by a decline in the oxidation rate. Overall, NFMOs had lower K values (0.0002–0.0036 $min^{-1}m^{-2}$) compared to those of other synthetic manganese oxides [42,44].

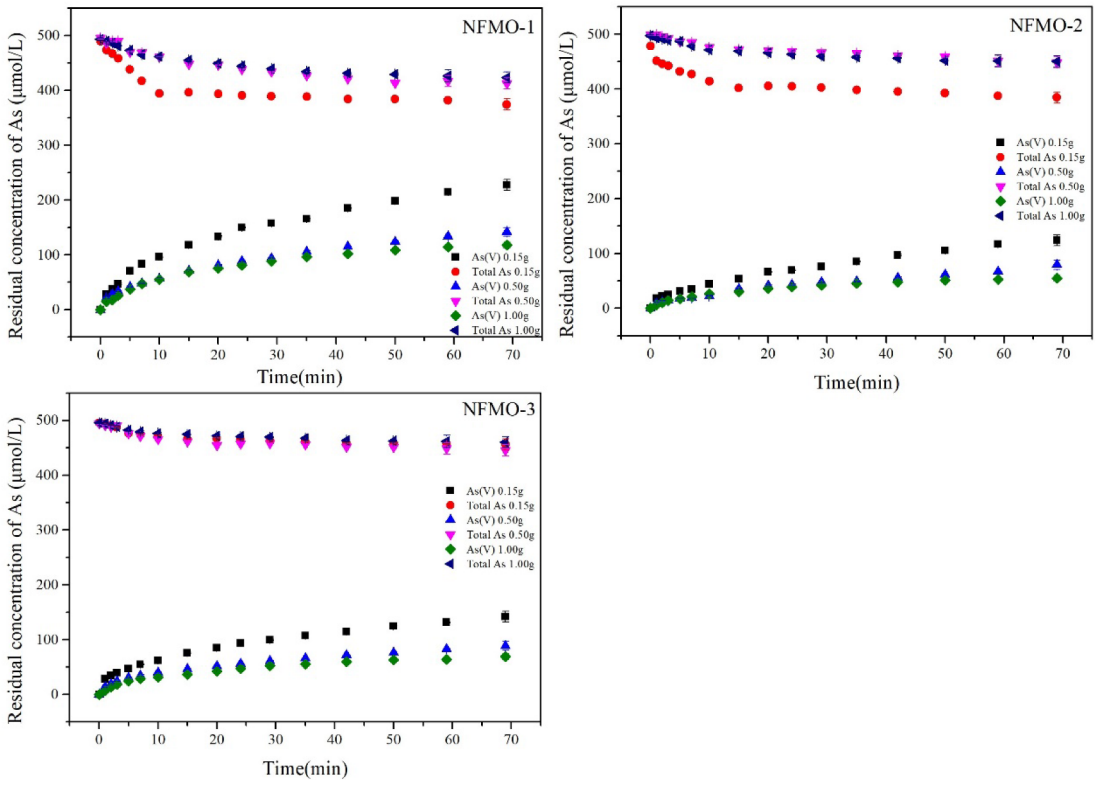

Fig. 3. The effects of sorbent dosage on As(III) oxidation by NFMOs. Initial As(III) concentration = 500 μmol/L, sorbent dosage = 0.15, 0.50, and 1.00 g, pH = 7.0 ± 0.05, and T = 25 °C.

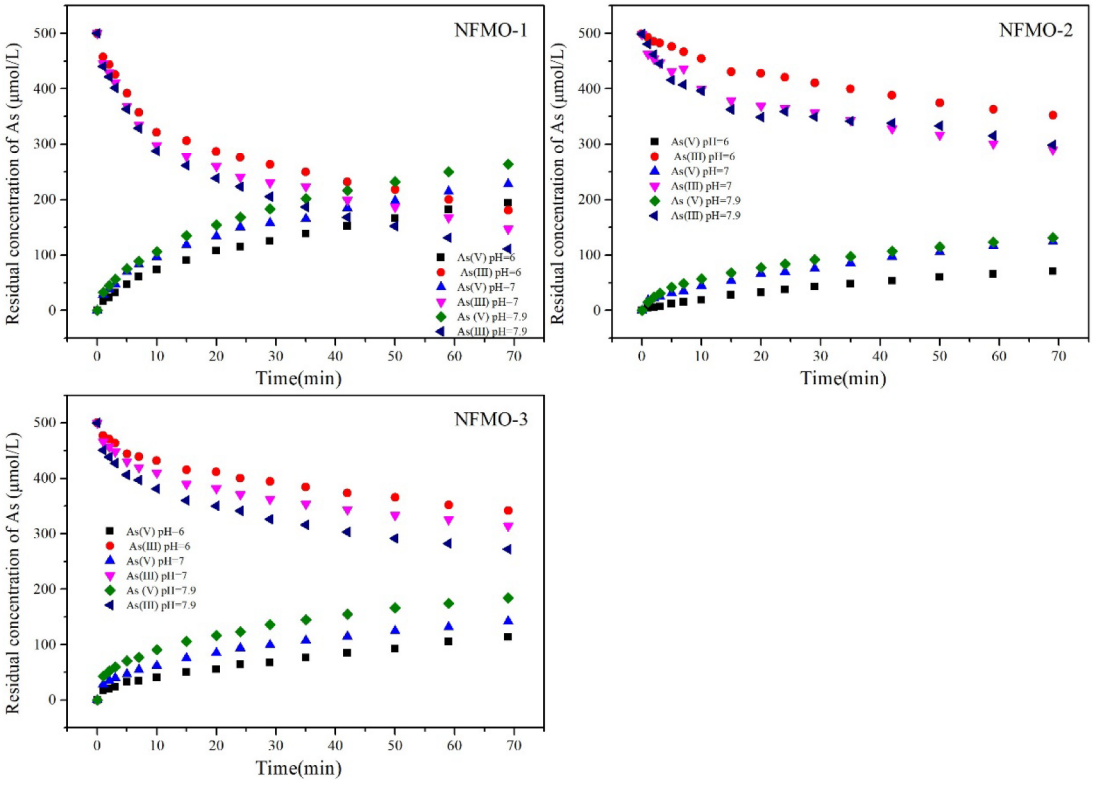

Fig. 4. The effects of pH on As(III) oxidation by NFMOs. Initial As(III) concentration = 500 μmol/L, sorbent dosage = 1.00 g, pH = 6.0, 7.0, and 7.9, and T = 25 °C.

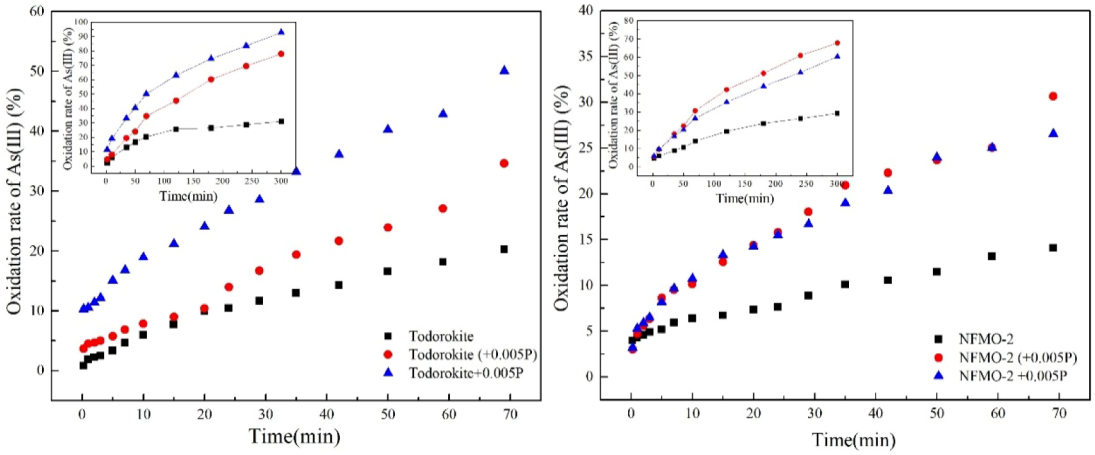

Fig. 5. The effects of pyrophosphate addition modes on the oxidation As (III) by synthetical todorokite and NFMO-2. Initial As (III) concentration = 500 μmol/L, sorbent dosage = 1.00 g, pH = 7.0 ± 0.05, and T = 25 °C. (+0.005P) means the 5 mmol/L $Na_4P_2O_7$ was added after todorokite or NFMO-2 suspended for 12 h; +0.005P means the 5 mmol/L $Na_4P_2O_7$ was added before todorokite or NFMO-2 suspended for 12 h.

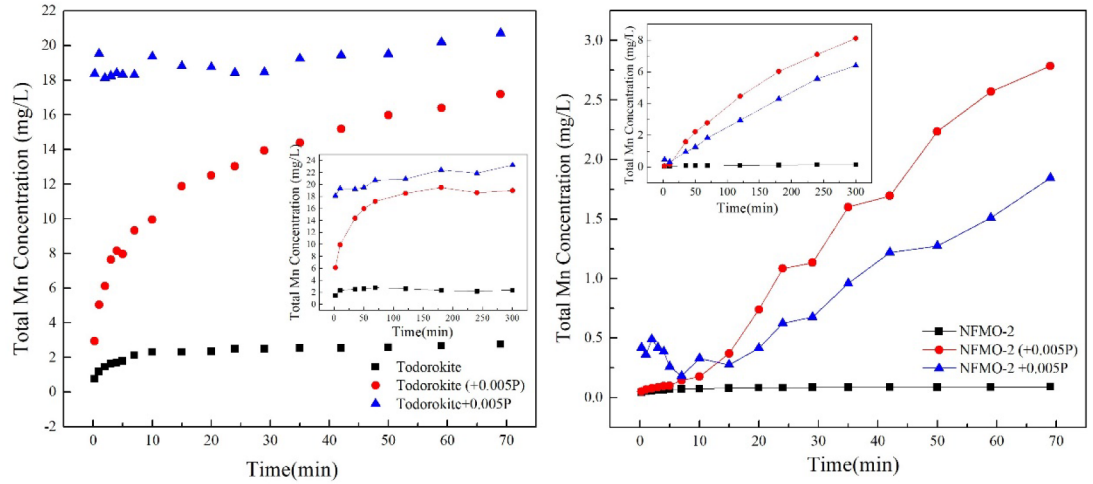

Fig. 6. The effects of pyrophosphate addition modes on the generation of total Mn from As(III) oxidation by synthetical todorokite and NFMO-2. Initial As (III) concentration = 500 μmol/L, sorbent dosage = 1.00 g, pH = 7.0 ± 0.05, and T = 25 °C. (+0.005P) means 5 mmol/L $Na_4P_2O_7$ was added after todorokite or NFMO-2 suspended for 12 h; +0.005P means 5 mmol/L $Na_4P_2O_7$ was added before todorokite or NFMO-2 suspended for 12 h.

3.4. Effect of sorbent dosage and pH on As(III) sorption

The influence of sorbent dosage and pH on the removal of As(III) by NFMOs was studied. With increasing sorbent dosages, As(V) concentration increased, while the total As concentration exhibited the opposite trend (Fig. 3). Hence it can be concluded that As(III) oxidation and adsorption efficiencies increased with higher sorbent dosages. Interestingly, sorbent dosage had no marked effect on NFMO-3 removal of As(III). This was most likely due to lower Mn content of NFMO-3 (20.93%), resulting in partial conversion of As(III) to As(V) [21].

As evident in Fig. 4, As(III) oxidation rates of all three NFMOs increased with increasing pH in a range of 6–7.9. NFMO-1, −2 and −3 oxidation rates were 54.2%, 28.2%, and 36.4%, respectively, at the highest tested pH of 7.9 and at 69 min. These results supported a literature finding, that the oxidation rate of As(III) by pyrolusite increased with an increase in the pH from 4.7 to 8 [45]. The availability of oxidation-adsorption sites on the surface of minerals may promote further oxidation of As(III) [25], and consequently enhance As(III) oxidation and adsorption efficiencies of the mineral. Moreover, As(V) adsorption declined with increasing pH (6–7.9), presenting a similar trend for As (V) sorption seen for the majority of Fe–Mn binary oxides [3,7]. Notably, $H_2AsO_4^-$ and $HAsO_4^{2-}$ gradually became the dominant As(V) species in the solution as the pH increased from 6 to 7.9. Rising coulombic repulsion between the As(V) species and negative surfaces of NFMOs (pHpzc = 3.56–6.35), eventually resulted in a decline of the As (V) sorption rate. This was attributed to inner-sphere complexation, and the formation of more intense chemical bonds between the oxyanion and adsorption sites [6]. As(III) remained neutral in the form of H_3AsO_3, suggesting that un-oxidised As(III) adsorption by NFMOs might be dominated by complex-specific adsorption [7], rather than electrostatic attraction. In addition, there were no obvious differences between As(III) sorption onto NFMO-2 at pH = 7 and at pH = 7.9, suggesting that when pH surpassed pHzpc (6.35), specific adsorption resulted in increased adsorption for both As(III) and As(V) [39].

3.5. Influence of pyrophosphate on As(III) oxidation

NFMO-2 was chosen for PP experiments due to a lower oxidation capacity and SSA relative to the other NFMOs; todorokite was the control. Fig. 5 illustrates the influence of PP addition protocols on As (III) oxidation by todorokite and NFMO-2. During first 69 min, the trends of As(III) oxidation rates by NFMO-2 with two PP addition protocols were similar; thereafter, the oxidation rate of PP addition within 12 h exceeded that of PP addition beyond 12 h. Meanwhile, As (III) oxidation rates were significantly higher when PP was added, than when PP was absent. After 5 h, oxidation rates of As(III) with

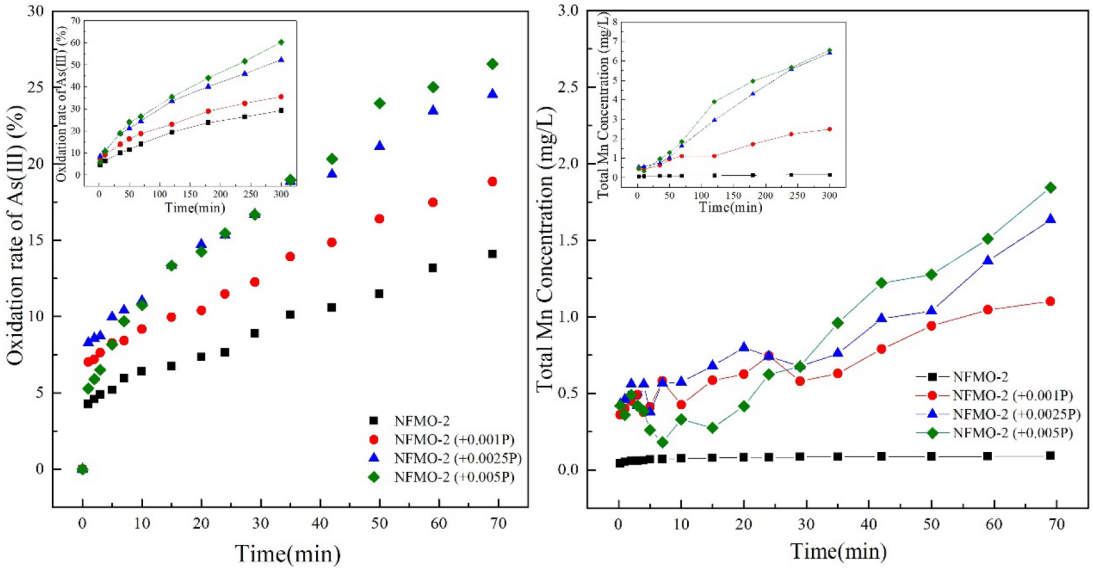

Fig. 7. The effects of pyrophosphate concentration on oxidation As (III) and generation of total Mn by NFMO-2. Initial As (III) concentration = 500 μmol/L, sorbent dosage = 1.00 g, pH = 7.0 ± 0.05, and T = 25 °C. (+0.001P), (+0.0025P), and (+0.005P) mean 1, 2.5, and 5 mmol/L $Na_4P_2O_7$ were added after NFMO-2 suspended for 12 h, respectively.

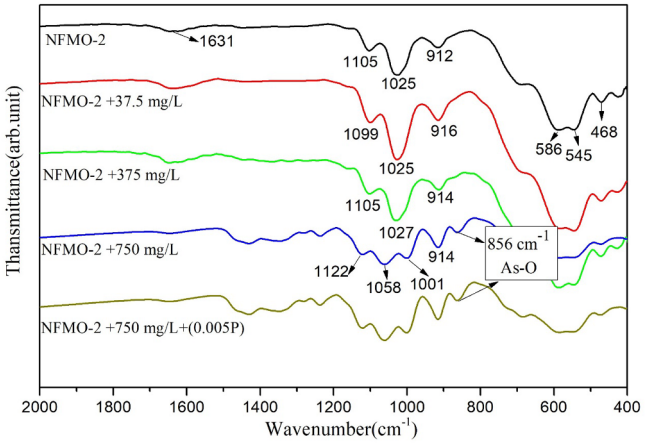

Fig. 8. FTIR spectra of NFMO-2 before and after As(III) adsorption. Initial As (III) concentration = 750 mg/L, sorbent dosage = 1.00 g, pH = 7.0 ± 0.05, and T = 25 °C. (+0.005P) means 5 mmol/L $Na_4P_2O_7$ was added after NFMO-2 suspended for 12 h.

pyrophosphate addition within 12 h, beyond 12 h, and those without PP, reached 60.29%, 67.74%, and 29.28%, respectively. This result demonstrated that the presence of PP considerably enhanced As(III) oxidation. Previous studies found that PP had a strong complexing effect on Mn(III) at neutral pH [46,47]. As Mn(III) is generated in the oxidation process, the number of Mn(III)-PP complexes increases with time [48,49]. These complexes were soluble in the reaction medium, thereby providing additional oxidation-adsorption sites on NFMOs and favouring As(III) oxidation. Interestingly, As(III) oxidation rates of todorokite with pyrophosphate addition within 12 h were significantly higher than the other two treatments. This was likely as a result of a high initial concentration of Mn in the PP-containing solution, (see Fig. 6), which could disrupt the equilibrium of Mn(II) − Mn(III) − Mn (IV) species in solution, in turn influencing As(III) oxidation [50,51]. Prior to oxidation taking place, PP forms complexes with Mn(III) present on the todorokite surface, leading to oxidation-adsorption site generation and enhanced As(III) oxidation.

Fig. 6 illustrates that the influence of PP addition protocols on the generation of total Mn during As(III) oxidation. For NFMO-2 without PP, the concentration of generated Mn remained relatively low. This result implies that Mn(III)/Mn(IV) generated from As(III) oxidation occupied the oxidation-adsorption sites on the adsorbent, thus inhibiting As(III) oxidation. When PP was present, concentrations of generated Mn followed similar trends as the oxidation rates of As(III). Total Mn concentrations with PP addition beyond 12 h were significantly higher than that with PP addition within 12 h. A possible explanation for this is an increase in the oxidation capacity of NFMO-2 with pyrophosphate addition beyond 12 h. For todorokite with PP addition beyond 12 h, the oxidation rate of As(III) increased, while the concentration of Mn reached a plateau after 69 min; this indicated that the bulk of the PP had formed complexes with Mn(III). Overall, as Mn (III) amounts on the surface of NFMO-2 were minimal, PP addition protocols had minor effects on the oxidation of As(III) and generation of total Mn. In view of these results, PP addition was performed beyond 12 h for the study on PP concentration effects.

The influence of PP concentrations (1, 2.5, and 5 mmol/L) on the oxidation of As(III) and generation of total Mn was studied, and the corresponding results are exhibited in Fig. 7. As(III) oxidation rates of NFMO-2 gradually increased during the 5 h experiment. A PP concentration of 5 mmol/L exhibited marginally higher oxidation rates than that of 2.5 mmol/L PP, but significantly higher than the other two treatments. Thus the optimal PP concentration in the NFMO-2 oxidation of As(III) was 5 mmol/L. Previous studies found that the total PP: Mn ratio was a vital factor in determining structural configuration of Mn(III)-PP complexes [52,53]. The $Mn(PP)_2^{5-}$ species is considered a relatively stable complex at neutral pH, but when the stability of complexing ligands decreases, Mn(III) disproportionation occurs [31,54]. Addition of 5 mmol/L PP resulted in considerably higher total Mn concentrations after 30 min, when compared to lower-concentration treatments, in keeping with the As(III) oxidation rate trends.

No Fe was detected in the NFMO-2 solution. This indicated that Fe oxides play an important role in adsorption, but do not participate in the oxidation step. This further confirmed that during As(III) removal by NFMO-2, Mn oxides exhibit a synergistic effect of oxidation and adsorption; while Fe oxides were only involved in As(III) sorption, thereby promoting oxidation of Mn oxide. This was consistent with previous studies that a synthesized Fe − Mn binary oxide presented an obvious synergistic effect. MnOx and FeOOH content were mainly responsible for As(III) oxidation and adsorbing formed As(V) during As (III) removal, respectively [55–56].

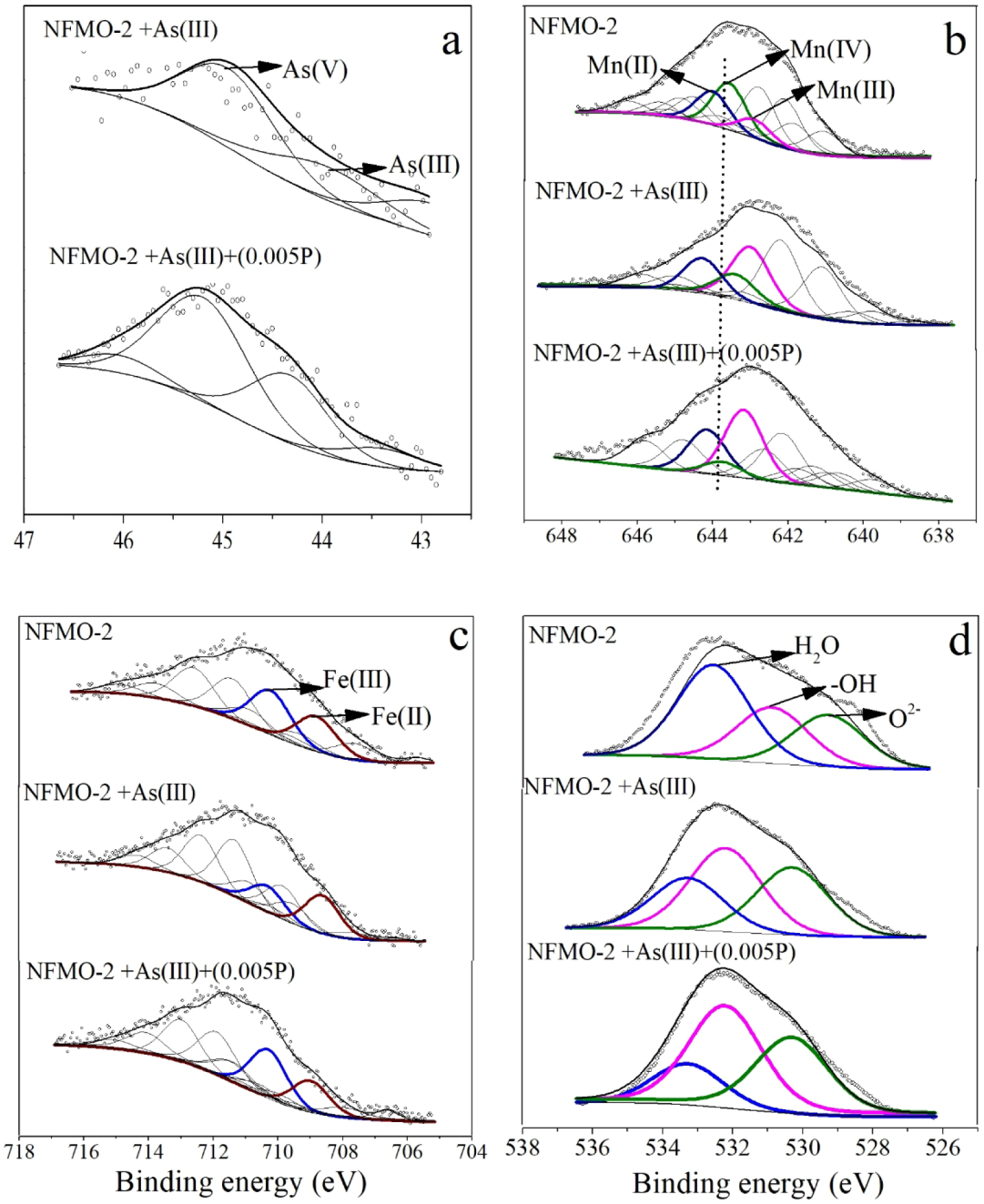

Fig. 9. XPS spectra of NFMO-2 before and after As(III) sorption: (a) As *3d* spectra, (b) Mn *2p* spectra, (c) Fe *3d* spectra and (d) O *1 s* spectra. Initial As (III) concentration = 750 mg/L, sorbent dosage = 1.00 g, pH = 7.0 ± 0.05, and T = 25 °C. (+0.005P) means 5 mmol/L $Na_4P_2O_7$ was added after NFMO-2 suspended for 12 h.

In summary, PP continuously forms complexes with Mn(III) generated from the conversion of Mn(IV) to Mn(III). This process greatly promotes the occurrence of the electron transfer reaction (Mn(IV) → Mn(III)). Then, large amounts of Mn(III)-PP complexes dissolve in the solution, resulting in the generation of additional oxidation-adsorption sites. Ultimately, As(III) oxidation rates and the total Mn concentration gradually increase. These results suggest that the limiting step of As(III) oxidation is the transformation of Mn(IV) to Mn(III).

3.6. Co-occurring redox reactions

FTIR spectra of NFMO-2 before and after reaction with As(III) at pH 7.0 are presented in Fig. 8. For NFMO-2, the band at 1630 cm^{-1} was ascribed to H_2O bending vibrations. Three peaks at 586, 545, and 468 cm^{-1} arose from Mn–O stretching vibrations of manganese oxides [57]. The strong band at 1025 cm^{-1} with shoulders at 1105 and 912 cm^{-1} may be assigned to the bending vibration of FeOH modes of feroxyhyte [58]. Subsequent to As(III) treatment, the peak at 1025 cm^{-1} weakened gradually with an increase in As(III) concentration. When the content of As(III) reached 750 mg/L, the peak at 1025 cm^{-1} was barely visible, accompanied with the appearance of two peaks at 1058 and 1001 cm^{-1}. This implies that the bending vibration of Fe-OH groups were susceptible to the presence of adsorbed As(III)/As (V) [21]. Moreover, a new peak was visible at 856 cm^{-1}, corresponding to an As–O stretching vibration [59]. This revealed that the majority of As(III) was oxidised to As(V), which replaced the surface hydroxyl groups of NFMO-2, and was bound as a surface complex [42]. Spectra of reactions containing PP showed no marked difference to those without

Table 3
The changes of content and valence for each element on NFMO-2 before and after As(III) sorption.

Combined state/ Valence	NFMO-2 (At.%)	NFMO-2 + As(III) (At. %)	NFMO-2 + As (+0.005P) (At.%)
C−C C=C C−H	85.54	69.56	63.19
C−OH C−O−C	0.290	10.45	20.23
C=O	7.410	12.57	7.910
O−C=O	6.760	7.420	8.670
O^{2-}	25.38	33.34	18.32
OH^-	28.39	41.23	26.83
H_2O	46.23	25.43	54.85
Fe(0)	5.18	2.02	2.150
Fe^{2+}	27.02	49.09	28.85
Fe^{3+}	67.80	48.89	69.00
Fe average	2.574	2.449	2.647
Mn^{2+}	22.87	34.16	35.79
Mn^{3+}	21.95	44.69	62.14
Mn^{4+}	55.18	21.15	2.070
Mn average	3.323	2.870	2.663
As(0)	–	0.00	0.00
As(III)-O	–	41.37	23.79
As(V)-O	–	58.63	76.21

(+0.005P) means 5 mmol/L $Na_4P_2O_7$ was added after NFMO-2 suspended for 12 h. Initial As (III) concentration = 750 mg/L, solid/liquid ratio = 1/300, pH = 7.0 ± 0.05, and T = 25 °C.

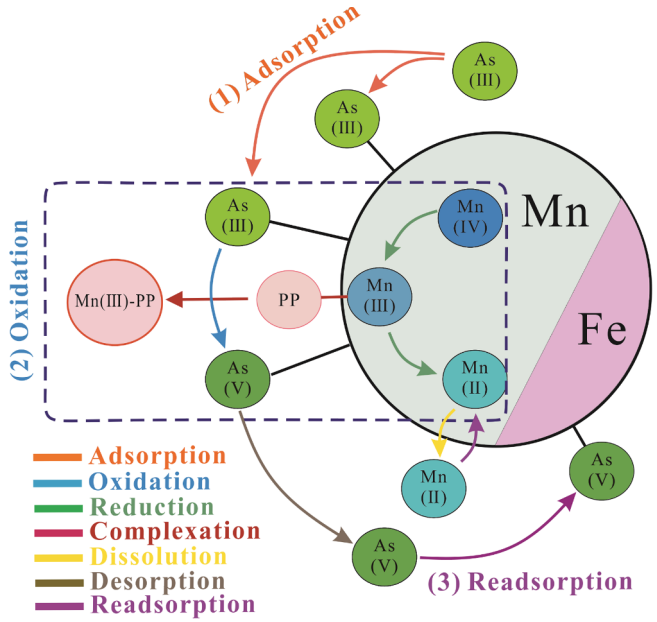

Fig. 10. The underlying mechanisms of As(III) oxidation and adsorption by natural Fe-Mn ore under pyrophosphate intervention.

PP, which indicates that PP had no effect on the occurrence of specific adsorption at the NFMO interface.

XPS analysis was used to further examine the chemical state and composition of NFMO-2 before and after As(III) sorption. The results of As 3d, Mn 2p, Fe 2p, O 1 s and electron binding energies are illustrated in Fig. 9. Changes in NFMO-2 surface compositions are shown in Table 3. The presence of an As3d core level peak revealed that As(III) and As(V) were successfully sorbed onto Fe-Mn ore (Fig. S5). As seen in Fig. 9a, As 3d peak positions (45.7 and 44.8 eV) and shapes were characteristic of As(V) and As(III), where binding energies were 45.2–45.6 eV and 44.3–44.5 eV, respectively [60]. This slight skewing of binding energies is attributable to As species sorbed onto the NFMO after oxidation of As(III) to As(V) [11]. According to the XPS analysis results, approximately 58.63% (no PP) and 76.21% (PP added) As(III) was oxidized to As(V) (Table 3). This further confirmed that NFMO has a high capacity for As(III) oxidation, especially in the presence of PP.

As presented in Fig. 9b, the binding energies at 644.2, 643.1, and 643.4 eV were assigned to Mn $2p_{3/2}$ spectra (Table S1) [61]. In order to further examine the Mn valence state, the peaks of Mn $2p_{3/2}$ were fitted according to a literature procedure [62]. Subsequent to reaction with As(III) and addition of PP, the average valence state of Mn decreased from 3.323 to 2.663 (Table 3). Percentages of Mn(IV) decreased dramatically from 55.18% to 2.07%; while Mn(III) and Mn(II) increased from 21.95% to 62.14%, and 22.87% to 35.79%, respectively. These results demonstrated that the significant decline of Mn(IV) can be attributed to the generation of PP complexes with Mn(III), which promotes conversion of Mn(IV) to Mn(III), and in turn oxidation of adsorbed As(III). Moreover, Fe 2p spectra were fitted with two peaks at 709.0 and 710.8 eV in Fig. 9c, which were characteristic of Fe(II) and Fe (III) (Table S1) [63]. As shown in Table 3, the average valence states of Fe were 2.574 and 2.647 before and after As(III) sorption and PP addition, respectively. No obvious changes in the percentages of Fe(II) (27.02%, 28.85%) and Fe(III) (67.80%, 69.00%) were observed. Therefore, the reduction of Mn(IV) and Mn(III) species was predominantly responsible for As(III) oxidation, while Fe oxide played a primary role in As sorption. The fitted O 1 s spectrum (Fig. 9d) exhibited three peaks at 529.6, 531.72 and 532.84 eV, characteristic of lattice oxygen (O^{2-}), hydroxyl (−OH), and adsorbed water (H_2O), respectively [60]. Following sorption under PP intervention, a distinct reduction in O^{2-} and -OH moieties was observed, from 25.38% to 18.32% and 28.39% to 26.83%, respectively (Table 3). These results suggested that As(V) gradually replaced the hydroxyl groups in NFMO during sorption, which was supported by findings in the FTIR analysis.

Consequently, the possible mechanism by which PP influences As (III) oxidation and adsorption by natural NFMOs, is depicted in Fig. 10. Firstly, As(III) are transported to the solid/water interface, then sorbed onto the surface of NFMO in the form of monodentate and bidentate complexes. Secondly, the reduction of Mn(IV) → Mn(III) → Mn(II) leads to effective As(III) oxidation. In the oxidation reaction, added PP complexes with Mn(III), promoting the conversion of Mn(IV) to Mn(III) and the oxidation of As(III) to As(V). Thirdly, the generated As(V) is successfully adsorbed onto NFMO. Moreover, partly formed As(V) is desorbed into the solution, accompanied with the dissolution of Mn (II) [14,25]. Finally, the As(V) in the solution is transported to the solid/water again and rapidly adsorbed by Fe oxides. While the Mn(II) is resorbed due to the negatively charged surface.

4. Conclusion

In this study, NFMO-2 with relatively high Fe content had a stronger adsorption capacity for As(III). However, As(III) oxidation rates of NFMO-1 with the highest Mn/Fe ratio reached 49.2% at 69 min, which was significantly higher than those of the other two NFMOs. Moreover, NFMO sorbent dosage had a remarkable effect on As(III) oxidation with higher Mn contents, but not with low-content ores. As(III) oxidation was strongly pH dependent, increasing as pH increased from 6 to 7.9. Furthermore, PP addition considerably enhanced As(III) oxidation by NFMO, and concentration of PP was a crucial factor in the process. These results indicated that the oxidation of As(III) to As(V) was attributed to the reduction of Mn(IV) and Mn(III) species in NFMO. Mn (II)-PP complexes dissolved in the solution, thus providing more oxidation adsorption sites to promote As(III) oxidation. Hence, addition of a liquid chelating agent, specifically PP, is a facile and effective method for enhancing As(III) oxidation performance of NFMO, making this a promising adsorbent system for practical wastewater treatment.

Declaration of Competing Interest

The authors declare that they have no known competing financial interests or personal relationships that could have appeared to influence the work reported in this paper.

Acknowledgements

This research was supported by the National Natural Science Foundation of China (Grant No. 41471407 and 51709255), China Postdoctoral Science Foundation (2017M622555).

Appendix A. Supplementary data

Supplementary data to this article can be found online at https://doi.org/10.1016/j.cej.2019.123040.

References

[1] J.F. Ferguson, J. Gavis, A review of the arsenic cycle in natural waters, Water Res. 6 (1972) 1259–1274.
[2] A. Sarkar, B. Paul, The global menace of arsenic and its conventional remediation – a critical review, Chemosphere 158 (2016) 37–49.
[3] J. Qi, G. Zhang, H. Li, Efficient removal of arsenic from water using a granular adsorbent: Fe–Mn binary oxide impregnated chitosan bead, Bioresource Technol. 193 (2015) 243–249.
[4] C. Wu, Q. Zou, S. Xue, J. Mo, W. Pan, L. Lou, M.H. Wong, Effects of silicon (Si) on arsenic (As) accumulation and speciation in rice (Oryza sativa L.) genotypes with different radial oxygen loss (ROL), Chemosphere 138 (2015) 447–453.
[5] C. Wu, Q. Zou, S. Xue, W. Pan, L. Huang, W. Hartley, J. Mo, M.H. Wong, The effect of silicon on iron plaque formation and arsenic accumulation in rice genotypes with different radial oxygen loss (ROL), Environ. Pollut. 212 (2016) 27–33.
[6] C. Shan, M. Tong, Efficient removal of trace arsenite through oxidation and adsorption by magnetic nanoparticles modified with Fe–Mn binary oxide, Water Res. 47 (2013) 3411–3421.
[7] G. Zhang, J. Qu, H. Liu, R. Liu, R. Wu, Preparation and evaluation of a novel Fe–Mn binary oxide adsorbent for effective arsenite removal, Water Res. 41 (2007) 1921–1928.
[8] T.S. Anirudhan, M.R. Unnithan, Arsenic(V) removal from aqueous solutions using an anion exchanger derived from coconut coir pith and its recovery, Chemosphere 66 (2007) 60–66.
[9] M. Walker, R.L. Seiler, M. Meinert, Effectiveness of household reverse-osmosis systems in a Western U.S. region with high arsenic in groundwater, Sci. Total Environ. 389 (2008) 245–252.
[10] M.A. Ferguson, M.R. Hoffmann, J.G. Hering, TiO_2 -Photocatalyzed As(III) Oxidation in Aqueous Suspensions: Reaction Kinetics and Effects of Adsorption, Environ. Sci. Technol. 39 (2005) 1880–1886.
[11] G. Zhang, A. Khorshed, J.P. Chen, Simultaneous removal of arsenate and arsenite by a nanostructured zirconium-manganese binary hydrous oxide: Behavior and mechanism, J. Colloid Interf. Sci. 397 (2013) 137–143.
[12] S. Dixit, J.G. Hering, Comparison of arsenic(V) and arsenic(III) sorption onto iron oxide minerals: implications for arsenic mobility, Environ. Sci. Technol. 37 (2003) 4182–4189.
[13] D. Mohan, C.U.P. Jr, Arsenic removal from water/wastewater using adsorbents–a critical review, J. Hazard. Mater. 142 (2007) 1–53.
[14] J. Chen, J. Wang, G. Zhang, Q. Wu, D. Wang, J. Chen, J. Wang, G. Zhang, Q. Wu, D. Wang, Facile fabrication of nanostructured cerium-manganese binary oxide for enhanced arsenite removal from water, Chem. Eng. J. 334 (2017) 1518–1526.
[15] M. Bissen, F.H. Frimmel, Arsenic – a Review, Part II: Oxidation of Arsenic and Its Removal in Water Treatment, Clean – Soil Air Water 31 (2003) 97–107.
[16] J.C.J. Gude, L.C. Rietveld, D.V. Halem, As(III) oxidation by MnO 2 during groundwater treatment, Water Res. 111 (2017) 41–51.
[17] S.J. Parikh, B.J. Lafferty, T.G. Meade, D.L. Sparks, Evaluating environmental influences on AsIII oxidation kinetics by a poorly crystalline Mn-oxide, Environ. Sci. Technol. 44 (2010) 3772–3778.
[18] V. Lenoble, C. Laclautre, B. Serpaud, V. Deluchat, J.C. Bollinger, As(V) retention and As(III) simultaneous oxidation and removal on a MnO_2 -loaded polystyrene resin, Sci. Total Environ. 326 (2004) 197–207.
[19] Y.B. Huang, L.L. Wang, S.X. Tu, X.Y. Liu, X.J. Li, Y. Li, Influence of various factors on arsenic removal using ferruginous manganese ore, Appl. Mech. Mater. 71–78 (2011) 2753–2758.
[20] Y. Huang, C. Huang, Q. Yang, L. Wang, S. Tu, C. Zhou, Preliminary mechanisms for arsenic removal by natural ferruginous manganese ore, Mater. Res. Innov. 19 (2015) S5-1313-S1315-1317.
[21] G.S. Zhang, H. Liu, J. Qu, W. Jefferson, Arsenate uptake and arsenite simultaneous sorption and oxidation by Fe-Mn binary oxides: influence of Mn/Fe ratio, pH, Ca^{2+}, and humic acid, J. Colloid Interf. Sci. 366 (2012) 141–146.
[22] G.S. Zhang, H. Liu, R. Liu, J. Qu, Adsorption behavior and mechanism of arsenate at Fe–Mn binary oxide/water interface, J. Hazard. Mater. 168 (2009) 820–825.
[23] S. Chakravarty, V. Dureja, G. Bhattacharyya, S. Maity, S. Bhattacharjee, Removal of arsenic from groundwater using low cost ferruginous manganese ore, Water Res. 36 (2002) 625–632.
[24] E. Deschamps, V.S.T. Ciminelli, W.H. Höll, Removal of As(III) and As(V) from water using a natural Fe and Mn enriched sample, Water Res. 39 (2005) 5212–5220.
[25] G.S. Zhang, J.H. Qu, H.J. Liu, R.P. Liu, G.T. Li, Removal mechanism of As(III) by a novel Fe-Mn binary oxide adsorbent: oxidation and sorption, Environ. Sci. Technol. 41 (2007) 4613–4619.
[26] G.S. Zhang, F. Liu, H. Liu, J. Qu, R. Liu, Respective role of Fe and Mn oxide contents for arsenic sorption in iron and manganese binary oxide: an X-ray absorption spectroscopy investigation, Environ. Sci. Technol. 48 (2014) 10316–10322.
[27] M.F.H. Jr, J.N. Moore, C.V. Putnis, A. Putnis, T. Kasama, D.D. Eberl, Direct observation of heavy metal-mineral association from the Clark Fork River Superfund Complex: Implications for metal transport and bioavailability, Geochim. Cosmochim. Ac. 69 (2005) 1651–1663.
[28] J.K. Klewicki, J.J. Morgan, Kinetic Behavior of Mn(III) Complexes of Pyrophosphate, EDTA, and Citrate, Environ. Sci. Technol. 32 (1998) 2916–2922.
[29] H. Cui, X. Liu, W. Tan, X. Feng, L. Fan, H.D. Ruan, Influence of Mn(III) Availability on the Phase Transformation From Layered Buserite to Tunnel-structured Todorokite, Clay. Clay Miner. 56 (2008) 397–403.
[30] J.K. Klewicki, J.J. Morgan, S.L.S. Stipp, P.V. Brady, K.V. Ragnarsdottir, L. Charlet, Dissolution of beta -MnOOH particles by ligands; pyrophosphate, ethylenediaminetetraacetate, and citrate, Geochim. Cosmochim. Ac. 63 (1999) 3017–3024.
[31] A. Qian, W. Zhang, C. Shi, C. Pan, D.E. Giammar, S. Yuan, H. Zhang, Z. Wang, Geochemical Stability of Dissolved Mn(III) in the Presence of Pyrophosphate as a Model Ligand: Complexation and Disproportionation, Environ. Sci. Technol. 53 (2019) 5768–5777.
[32] X. Han, Y.F. Wang, X.K. Tang, H.T. Ren, S.H. Wu, S.Y. Jia, Lepidocrocite-catalyzed Mn(II) oxygenation by air and its effect on the oxidation and mobilization of As(III), Appl. Geochem. 72 (2016) 34–41.
[33] R.M. Weaver, M.F. Hochella, The reactivity of seven Mn-oxides with Cr^{3+}aq: A comparative analysis of a complex, environmentally important redox reaction, Am. Mineral. 88 (2003) 2016–2027.
[34] X.H. Feng, W.F. Tan, F. Liu, J.B. Wang, H.D. Ruan, Synthesis of Todorokite at Atmospheric Pressure, Chem. Mater. 16 (2004) 4330–4336.
[35] N. Kijima, H. Yasuda, T. Sato, Y. Yoshimura, Preparation and Characterization of Open Tunnel Oxide α-MnO_2 Precipitated by Ozone Oxidation, J. Solid State Chem. 159 (2001) 94–102.
[36] W.F. Tan, F. Liu, Y.H. L, J.Z. He, X.Y. Li, Mineralogy of manganese in iron-manganese nodules of several soils in China, Acta Pedologica Sinica 37 (2000) 192-201 (in Chinese).
[37] J. Hong, L. Liu, Y. Luo, W. Tan, G. Qiu, F. Liu, Photochemical oxidation and dissolution of arsenopyrite in acidic solutions, Geochim. Cosmochim. Ac. 239 (2018) 173–185.
[38] M. Ajmal, R.A.K. Rao, B.A. Siddiqui, Adsorption studies and the removal of dissolved metals using pyrolusite as adsorbent, Environ. Monit. Assess. 38 (1995) 25–35.
[39] F. Chang, J. Qu, H. Liu, R. Liu, Z. Xu, Fe-Mn binary oxide incorporated into diatomite as an adsorbent for arsenite removal: preparation and evaluation, J. Colloid Interf. Sci. 338 (2009) 353–358.
[40] R.A. Root, S. Dixit, K.M. Campbell, A.D. Jew, J.G. Hering, P.A. O'Day, Arsenic sequestration by sorption processes in high-iron sediments, Geochim. Cosmochim. Ac.71 (2007) 5782–5803.
[41] M.L. Pierce, C.B. Moore, Adsorption of arsenite and arsenate on amorphous iron hydroxide, Water Res. 16 (1982) 1247–1253.
[42] D. Ociński, I. Jacukowicz-Sobala, P. Mazur, J. Raczyk, E. Kociołek-Balawejder, Water treatment residuals containing iron and manganese oxides for arsenic removal from water – Characterization of physicochemical properties and adsorption studies, Chem. Eng. J. 294 (2016) 210–221.
[43] M. Ginder-Vogel, G. Landrot, J.S. Fischel, D.L. Sparks, Quantification of rapid environmental redox processes with quick-scanning x-ray absorption spectroscopy (Q-XAS), P. Natl. Acad. Sci. USA. 106 (2009) 16124.-16128.
[44] Irina V. Chernyshova, S. Ponnurangam, P. Somasundaran, Effect of nanosize on catalytic properties of ferric (hydr)oxides in water: Mechanistic insights, J. Catal. 282 (2011) 25-34.
[45] X.J. Li, C.S. Liu, F.B. Li, Y.T. Li, L.J. Zhang, C.P. Liu, Y.Z. Zhou, The oxidative transformation of sodium arsenite at the interface of α-MnO_2 and water, J. Hazard. Mater. 173 (2010) 675–681.
[46] W. Yun, A.T. Stone, Phosphonate- and carboxylate-based chelating agents that solubilize (hydr)oxide-bound MnIII, Environ. Sci. Technol. 42 (2008) 4397–4403.
[47] G.W.L. Iii, A.S. Madison, A. Mucci, B. Sundby, V.E. Oldham, A kinetic approach to assess the strengths of ligands bound to soluble Mn(III), Mar. Chem. 173 (2015) 93–99.
[48] K. Toyoda, B.M. Tebo, Kinetics of Mn(II) oxidation by spores of the marine Bacillus sp. SG-1, Geochim. Cosmochim. Ac. 189 (2016) 58–69.
[49] W. Liu, B. Sun, J. Qiao, X. Guan, Influence of Pyrophosphate on the Generation of Soluble Mn(III) from Reactions Involving Mn Oxides and Mn(VII), Environ. Sci. Technol. 53 (2019) 10227–10235.
[50] J.P. Lefkowitz, A.A. Rouff, E.J. Elzinga, Influence of pH on the reductive transformation of birnessite by aqueous Mn(II), Environ. Sci. Technol. 47 (2013) 10364–10371.
[51] E.J. Elzinga, Reductive transformation of birnessite by aqueous Mn(II), Environ. Sci. Technol. 45 (2011) 6366–6372.
[52] O.W. Duckworth, G. Sposito, Siderophore – Manganese(III) Interactions II. Manganite Dissolution Promoted by Desferrioxamine B, Environ. Sci. Technol. 39 (2005) 6045–6051.
[53] J.E. Kostka, G.W. Luther, K.H. Nealson, Chemical and biological reduction of Mn (III)-pyrophosphate complexes: potential importance of dissolved Mn (III) as an environmental oxidant, Geochim. Cosmochim. Ac. 59 (1995) 885–894.
[54] Q. Li, L. Xie, Y. Jiang, J.D. Fortner, K. Yu, P. Liao, C. Liu, Formation and stability of NOM-Mn(III) colloids in aquatic environments, Water Res. 149 (2019) 190–201.
[55] G.S. Zhang, H. Liu, F.D. Liu, H.J. Liu, J.H. Qu, R.P. Liu, Respective role of Fe and Mn oxide contents for arsenic sorption in iron and manganese binary oxide: an X-ray absorption spectroscopy investigation, Environ. Sci. Technol. 48 (2014) 10316–10322.

[56] H.T. Ren, S.Y. Jia, S.H. Wu, Y. Liu, C. Hua, X. Han, Abiotic oxidation of Mn(II) induced oxidation and mobilization of As(III) in the presence of magnetite and hematite, J. Hazard. Mater. 254–255 (2013) 89–97.
[57] S.J. Parikh, J. Chorover, FTIR Spectroscopic Study of Biogenic Mn-Oxide Formation by Pseudomonas putida GB-1, Geomicrobiol. J. 22 (2005) 207–218.
[58] L. Mei, L. Liao, Z. Wang, C. Xu, Interactions between Phosphoric/Tannic acid and different forms of FeOOH, Adv. Mater. Sci. Eng. ID (2015) 250836.
[59] S. Goldberg, C.T. Johnston, Mechanisms of arsenic adsorption on amorphous oxides evaluated using macroscopic measurements, vibrational spectroscopy, and surface complexation modeling, J. Colloid Interf. Sci. 234 (2001) 204–216.
[60] Y. Yang, C. Zhang, L. Yang, J.P. Chen, Cerium oxide modified activated carbon as an efficient and effective adsorbent for the rapid uptake of arsenate and arsenite: material development and study of performance and mechanisms, Chem. Eng. J. 315 (2017) 630–638.
[61] E.S. Ilton, J.E. Post, P.J. Heaney, F.T. Ling, S.N. Kerisit, XPS determination of Mn oxidation states in Mn (hydr)oxides, Appl. Surf. Sci. 366 (2016) 475–485.
[62] H.W. Nesbitt, G.W. Canning, G.M. Bancroft, XPS study of reductive dissolution of 7Å-birnessite by H_3AsO_3, with constraints on reaction mechanism, Geochim. Cosmochim. Ac. 62 (1998) 2097–2110.
[63] M.C. Biesinger, L.W.M. Lau, A.R. Gerson, R.S.C. Smart, Resolving surface chemical states in XPS analysis of first row transition metals, oxides and hydroxides: Sc, Ti, V, Cu and Zn, Appl. Surf. Sci. 257 (2010) 887–898.